ELSEVIER

Applied Catalysis B: Environmental 22 (1999) 35–47

APPLIED CATALYSIS B: ENVIRONMENTAL

Effects of water vapor and sulfur dioxide on the performance of Ce–Ag-ZSM-5 for the SCR of NO with CH_4

Zhijiang Li, Maria Flytzani-Stephanopoulos *

Department of Chemical Engineering, Tufts University, Medford, MA 02155, USA

Received 22 July 1998; received in revised form 8 March 1999; accepted 15 March 1999

Abstract

The activity and stability of Ce–Ag-ZSM-5 catalysts for the selective catalysts reduction (SCR) of NO with CH_4 in the presence of water vapor and SO_2 was studied in this work. Pre-steaming or wet aging of the catalyst in the reaction gas mixture caused a drop in activity. The loss of catalytic activity was partially irreversible and with an increase of water content and/or temperature the irreversible loss became predominant. However, at all tested conditions, including at a temperature of 600°C and in the presence of 8% water, the catalyst was capable of retaining a stable NO conversion to N_2 during a 100 h-long test. In the presence of SO_2, the activity of Ce–Ag-ZSM-5 decreased significantly at 500°C, but it was recovered by increasing the temperature to above 550°C. NO uptake measurements and characterization of steamed, sulfated and reaction-aged catalyst samples by XRD, HRTEM, STEM/EDS and XPS were carried out to study the deactivation. The NO uptake capacity of pre-steamed samples decreased as steaming temperature was raised from 400°C to 600°C, but that of pre-sulfated catalysts increased with temperature reaching 80% of the fresh material-uptake capacity after the 600°C-sulfation. Water induced sintering of silver. This, in turn, caused the lower NO uptake and the irreversible loss of the SCR activity observed after severe steaming. In the case of SO_2, inhibition of the SCR reaction at low temperatures is caused by SO_2 adsorption on active sites. However, this is fully reversible with temperature. No permanent loss of activity due to structural modification took place in SO_2-containing reaction gases. ©1999 Elsevier Science B.V. All rights reserved.

Keywords: Selective reduction of NO; Methane; ZSM-5; Silver; Cerium; Aging; Water and SO_2 effects

1. Introduction

The selective catalytic reduction (SCR) of NO_x with hydrocarbons in the presence of excess oxygen has received much attention recently because of its potential application to mobile lean-burn engines. The use of methane as the reductant would apply to CNG-engines and vehicles. Several metal ion-exchanged zeolites, such as Co- [1,2], Mn- [1], Ga- [3,4], In- [5,6], Pd- [7,8], and Ce–Ag-ZSM-5 [9] have been shown to be active for the SCR of NO with CH_4. However, water vapor and sulfur dioxide are typically present in combustion exhausts and may cause severe deactivation of catalyst for the SCR reaction. Thus, it is important for practical application that any NO_x SCR catalyst be capable of retaining its activity for a reasonably long time in the presence of both poisons.

Studies on the H_2O- and SO_2-induced deactivation of catalysts for the SCR of NO by CH_4 are scarce and not fully documented in the literature. In Table 1, the dry and wet performance of several ZSM-5-based

* Corresponding author.; e-mail: mstephanopoulos@infonet.tufts.edu

0926-3373/99/$ – see front matter ©1999 Elsevier Science B.V. All rights reserved.
PII: S0926-3373(99)00036-3

Table 1
Comparison of the dry and wet performance of ZSM-5 catalysts for the SCR of NO by CH_4

Catalyst	Si/Al	Metal (wt.%)	S.V. (h^{-1})	NO (ppm)	CH_4/NO (molar)	H_2O (mol%)	T (°C)	NO conversion to N_2 (%)		Ref.
								Dry	Wet	
Ga-HZSM-5	12	4.2	30 000	1610	0.62	2	500	40	13	[3]
			30 000	1610	0.62	2	550	33	16	
In-HZSM-5	12	NA[a]	12 000	1000	1	–	500	75	–	[4]
			30 000	1000	1	10	500	NA	10	
			30 000	1000	1	10	600	NA	8	
Pd-HZSM-5	25	1.0	35 000	2000	0.5	10	500	38	27	[7]
Co-ZSM-5	13.6	4.0	30 000	820	1.2	2	450	47	23	[10]
	11	5.0	30 000	850	1.2	2	500	39	30	[11]
			30 000	850	1.2	2	600	21	22	

[a] NA: not available.

CH_4-SCR catalysts is compared. It is clear that the presence of water vapor decreases the activity of all these catalysts. The most significant impact was reported on Ga-HZSM-5 [3] and In-HZSM-5 [4], over which up to 70% drop of dry NO conversion to N_2 was found with addition of 2% and 10% H_2O into the feed gas stream. After removal of water, the activity of these two catalysts was recovered only partially. Co-ZSM-5 [10,11] and Pd-HZSM-5 [7] exhibit better resistance to water poisoning, especially the Co-ZSM-5 material whose activity was reported to be fully restored after removal of water. However, the activity of these catalysts in wet conditions is still too low for practical application. In the presence of 53 ppm SO_2, the activity of Co-ZSM-5 was reported to drop significantly both under dry and wet conditions [11]. The coexistence of SO_2 and H_2O in the feed gas stream was more detrimental than either of these two gases alone.

Catalyst deactivation due to the presence of H_2O and SO_2 can be caused by adsorption of H_2O and SO_2 on active site and by changes of catalyst structure upon exposure to these gases at elevated temperatures. For Co-ZSM-5, competition between H_2O and NO molecules for the active Co sites and the poisoning of these sites by SO_2 have been invoked to explain the decrease of catalyst activity [11]. However, little attention has been paid to the issue of structural changes. In their studies of hydrothermal stability of Cu-ZSM-5 for the direct NO decomposition, Zhang et al. [12,13], Kucherov et al. [14] and Grinsted et al. [15] have reported that zeolite dealumination and agglomeration of copper forming CuO particles occurred when the catalyst was exposed to water-containing gas mixtures at elevated temperatures. These structural changes were found to contribute to the irreversible loss of catalyst activity.

Recently, we have reported that Ce-promoted Ag-ZSM-5 is very active for the SCR of NO by CH_4 over the wide temperature window of 400–650°C [9]. A small amount of cerium (1.0–1.5 wt.%) in Ag-ZSM-5 gave the maximum promotion, while the conversion of NO to N_2 increased linearly with the silver exchange level up to ~60%. The dispersed silver state, mainly in the form of Ag^+ ions, was more active for the SCR reaction than metallic silver nanoparticles, which selectively catalyze the deep oxidation of methane [16–19]. Previous reports of the SCR activity of silver catalysts were limited to other organic reductants, but not methane. For example, silver supported on alumina, TiO_2–ZrO_2 and mordenite has been studied for the SCR of NO with propene, ethanol, 2-propanol and acetone [20–26]. These studies have shown that silver-based catalysts are among the most active and durable catalysts for NO reduction in the presence of both water vapor and sulfur dioxide when higher hydrocarbons or oxygenates are used as reductants. Addition of 10% H_2O and 80–200 ppm SO_2 has little effect on the activity of Ag/Al_2O_3 at temperatures higher than 400–450°C [21,24]. An enhancement was even reported for the SCR of NO with 2-propanol and acetone over Ag/TiO_2–ZrO_2 when water was present [25].

However, the silver catalysts reported in the literature were not active for the SCR of NO using CH_4

as the reductant. In a previous paper, we reported that Ag-ZSM-5 also has low activity for this reaction up to 600°C [9]. It is only in the presence of cerium that Ag-ZSM-5 becomes a very active catalyst for the SCR of NO by CH_4. In this paper, we report on the effects of water vapor and/or sulfur dioxide on the performance of the Ce–Ag-ZSM-5 for CH_4-SCR of NO. The activity/selectivity of the catalyst in H_2O- and SO_2-containing gas streams and the performance recovery after removal of these two gases were evaluated. NO uptake measurements and characterization of steamed, sulfated and aged catalyst samples by XRD, STEM/EDX, HRTEM and XPS were used to elucidate the observed catalyst performance.

2. Experimental

2.1. Sample preparation

Detailed procedures for preparation of ion-exchanged Ce–Ag-ZSM-5 catalysts were described in a previous paper [9]. Na-ZSM-5 with Si/Al = 13 (obtained from the Davison Chemical Division, W.R. Grace , Lot No. SMR5-5829-0994) was used as the parent zeolite. The samples were prepared by first exchanging the Na-ZSM-5 with aqueous solutions of cerium(III) nitrate and then silver(I) nitrate. Cerium exchange was carried out at 80°C for 2 h using 200 ml 0.0003–0.01 M cerium(III) nitrate solution to exchange 2 g zeolite. The sample was then filtered, rinsed with 200 ml deionized water, dried at 110°C overnight in air, and calcined at 500°C in air for 2 h. Following this, Ag exchange took place in a 0.001–0.01 M silver(I) nitrate solution at room temperature in the dark for 24 h. For higher loadings, the exchange was repeated 2–3 times prior to rinsing. The elemental composition of the as-prepared samples was determined by inductively coupled plasma emission spectrometry (ICP, Perkin-Elmer Plasma 40). Table 2 lists the samples prepared in this work, their corresponding ICP analysis and charge balance. In Table 2 the number in parenthesis next to each element indicates the percent exchange level, assuming that each Ag^+ ion exchanges one Na^+ ion and each Ce^{3+} ion exchanges three Na^+ ions. The latter is hardly possible in high Si/Al-zeolites, so it is used only as an upper limit in evaluating charge balances. The charge balance for each sample was computed as (3Ce + Ag + Na)/Al. This calculation may show an artificially high value, i.e. (3Ce + Ag + Na)/Al greater than 1. On the other hand, protonation of some sites may be inferred by a charge balance less than unity.

Table 2
Preparation of ion-exchanged Ag- and Ce–Ag-ZSM-5 catalysts[a]

Catalyst	Si/Al	Ce/Al	Ag/Al	Na/Al	Charge balance
Ag(77)-ZSM-5	12.4	–	0.77	0.08	0.85
Ce(21)-Ag(42)-ZSM-5	11.7	0.07	0.42	0.33	0.99
Ce(24)-Ag(78)-ZSM-5	14.0	0.08	0.78	0.01	1.03
Ce(49)-Ag(79)-ZSM-5	12.8	0.16	0.79	0.00	1.28

[a] (1) Na-ZSM-5 (Si/Al = 13.8) was supplied by the Davison Chemical Division, W.R. Grace, Lot No.: SMR 5-5829-0994. (2) Ce ion exchange was performed at 80°C for 2 h with aqueous solution of $Ce(NO_3)_3 \cdot 6H_2O$ (Aldrich, Milwaukee, WI). (3) Ag ion exchange was performed at room temperature in the dark with aqueous solution of $AgNO_3$ (Johnson Matthey Electronics, Ward Hill, MA.). (4) Si, Al, Ce, Ag, Na contents were measured by ICP. (5) Charge balance was calculated as (3Ce + Ag + Na)/Al.

2.2. SCR tests in a microreactor

The activity of the catalyst in the presence and absence of H_2O and SO_2 was measured in the fixed-bed microreactor assembly described in [9]. A HP-5890 gas chromatograph (GC) equipped with a thermal conductivity detector (TCD) and a 10 ft, 1/8 in. O.D. 5A molecular sieve column operated at 40°C was used to separate O_2, N_2, CH_4, NO and CO.

The effect of water vapor on the activity of Ce–Ag-ZSM-5 was examined in two modes: (i) SCR of pre-steamed samples under dry conditions, and (ii) SCR of fresh samples in isothermal dry–wet cycles. In the first mode, the sample was first heated in He (Airco, Grade 4.7) at 500°C for 2 h (standard pre-treatment) and then cooled or heated to 400°C, 500°C or 600°C. After reaching the desired temperature, a gas mixture of 14.1% H_2O in He was switched in for 24 h. After cooling to room temperature, a reacting gas mixture of 0.5% NO, 0.5% CH_4, 2.5% O_2, bal. He was introduced into the reactor at a space velocity of 7500 h^{-1} (STP). The reaction temperature was then raised stepwise from 350°C to 650°C in 50°C per step. Only steady-state data were collected at each temperature. In the second mode, after the standard pre-treatment,

the temperature was cooled or raised to 400°C, 500°C or 600°C in the reacting gas mixture and kept constant at each temperature while water was alternatively added into and removed from the feed gas stream. Typically, each cycle was 20 h-long and four cycles were performed in each experiment. The gas mixture used in the cyclic experiments was 0.5% NO, 0.5% CH_4, 2.5% O_2, (x% H_2O), bal. He at a space velocity of 7500 h^{-1} (STP).

The effect of SO_2 alone and in combination with H_2O was examined at 500°C and 600°C in a manner similar to the cyclic tests described above. Two experimental conditions were used in these tests: 0.5% NO, 0.5% CH_4, 2.5% O_2, (75 ppm SO_2), bal. He at a space velocity of 7500 h^{-1} (STP) and 0.1% NO, 0.2% CH_4, 2.5% O_2, (5% H_2O, 50 ppm SO_2), bal. He at a space velocity of 30 000 h^{-1} (STP). In all experiments, the product gases did not contain any CO. Thus, the amount of N_2 produced and of CH_4 consumed during reaction was used to calculate, respectively, the conversion of NO to N_2 and of CH_4 to CO_2.

2.3. Catalyst characterization

Selected fresh, steamed, sulfated and aged catalyst samples were characterized by NO-uptake and by XRD, HRTEM, STEM/EDS and XPS analyses. The fresh samples were heat-treated in air at 500°C for 2 h. Steaming was performed in the fixed-bed microreactor with 14.1% H_2O in He at 400°C, 500°C or 600°C for 24 h after the standard pre-treatment. Sulfation was performed with 500 ppm SO_2 in He at 400°C, 500°C or 600°C for 1 h in a thermogravimetric analyzer (described below). Two types of aged samples were studied in this work: dry gas-aged and wet gas-aged, obtained by exposing the catalyst samples, respectively, to a dry gas mixture of 0.5% NO, 0.5% CH_4, 2.5% O_2, bal. He and a wet gas stream of 0.5% NO, 0.5% CH_4, 2.5% O_2, 14.1% H_2O, bal. He at 500°C for 24 h following the standard pre-treatment.

The NO uptake capacity of fresh, steamed and sulfated Ce–Ag-ZSM-5 samples was measured in a Cahn 121 thermogravimetric analyzer (TGA). The TGA has a resolution of 10^{-7} g and is equipped with four mass flow controllers (Tylan General, FC-260) and a power supply/readout unit. For fresh and steamed samples, about 10 mg of the catalyst powder was loaded in the TGA and heated to 500°C in He. After purging for 1 h, the temperature was lowered to 300°C and 0.476% NO in He was switched in to start the adsorption test. The inlet gas was then switched between NO/He and pure He after stable weight was obtained in either condition to study the reversibility of the adsorption. Typically, two cycles of consecutive adsorption and desorption were performed. To measure NO uptake on sulfated samples, the samples were cooled or heated to 400°C, 500°C or 600°C following the 500°C-purging in He. After that, 500 ppm SO_2 in He was passed through the TGA reactor for 1 h to sulfate the sample which was followed by cooling to 300°C in He. Not all the SO_2 was desorbed in this step. After stable weight was obtained, the NO/He or pure He gas was introduced into the TGA sequentially to carry out the isothermal adsorption–desorption experiment as described above. A flow rate of 100 ml min^{-1} (STP) was used in all uptake experiments.

A Rigaku RU-300 X-ray diffractometer (XRD) equipped with a rotating copper anode source was used to identify the crystalline phases in catalyst samples. The X-ray source was operated at 60 kV and 300 mA. Samples in fine powder form were directly pressed onto a 3/4 by 5/8 in. frosted area etched on a glass holder. The diffraction patterns were taken in the 2θ range of 5–60° at a scan speed of 1° min^{-1} and a resolution of 0.02°.

A JEOL 2010 high resolution transmission electron microscope (HRTEM) operated at 200 kV was used to study the morphology of catalyst samples. The TEM has an ultimate point-to-point resolution of 0.19 nm and is equipped with a X-ray detector for elemental analysis of selected sample areas. The catalyst samples were coated with carbon and supported on a 200 mesh copper grid prior to the TEM analysis.

A VG HB603 scanning transmission electron microscope (STEM) equipped with an energy dispersive X-ray detector (EDS) was used to obtain elemental distributions in catalyst samples. The samples were supported on a 200-mesh copper grid in the STEM chamber without coating. The distributions of Ag, Ce, Si, Al and O in the catalyst samples were obtained simultaneously with a spot size of 0.5 nm × 1 nm and a magnification of 5×10^5.

A Perkin-Elmer Model 5100 X-ray photoelectron spectroscope (XPS) was used here to determine elemental ratios on the surface of the catalyst samples. The Al Kα anode X-ray source was operated at

300 W. A layer of catalyst sample in powder form was pressed on a copper adhesive tape mounted on the sample holder. Each sample was exposed to the X-ray beam for about 40 min for data acquisition. Atomic ratios of silver and cerium to silicon in the surface region (3–4 nm) of the zeolite particles were determined based on the core level spectra of Ag, Ce and Si. Since reduction of silver by the X-ray beam from 1+ to 0 state may have occurred during the exposure of the samples to the beam, (as indicated by the color change of the samples from white to dark gray), XPS could not be used to quantify the fraction of silver in different oxidation states.

3. Results and discussion

3.1. Effect of water on the performance of Ce–Ag-ZSM-5

3.1.1. Activity of pre-steamed samples

The SCR-performance of 400°C, 500°C and 600°C-steamed Ce(24)–Ag(78)-ZSM-5 is shown in Fig. 1(a) and (b) in terms of NO conversion to N_2 and CH_4 conversion to CO_2, respectively. This is compared to the fresh (as prepared) sample. As can be seen from this figure, a 24 h-long pre-treatment of the sample with water vapor at temperatures above 500°C has a dramatic effect on the catalyst performance. Both the NO and the CH_4 conversion decreased significantly after the 500°C and 600°C-steaming of the sample. The largest drop of NO conversion over the 500°C and 600°C-steamed samples is seen at 500°C, causing the 'volcano-shaped' profile of NO conversion versus temperature to disappear (Fig. 1(a)). Fig. 1(b) shows the corresponding CH_4 conversion profiles. The light-off temperature (at 50% conversion of CH_4) shifted from 475°C for the fresh sample to 500°C and 600°C for the 500°C and 600°C-steamed samples, respectively. The results indicate that pre-steaming at temperatures ≥500°C causes a decrease of the SCR activity of Ce–Ag-ZSM-5 and also suppresses methane combustion. The latter is manifested by the lack of improvement of CH_4 conversion after steaming, as shown in Fig. 1(b). Therefore, steaming causes a loss to both functions of the catalyst (SCR and CH_4 combustion).

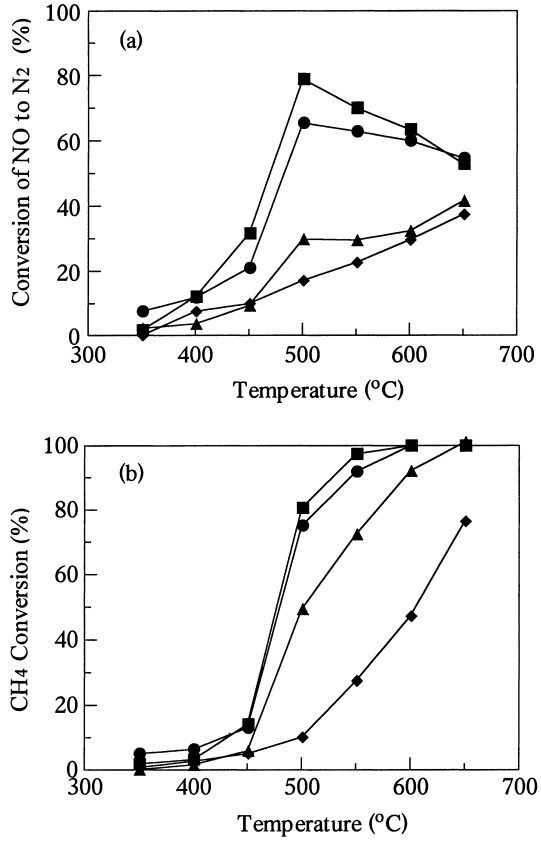

Fig. 1. Effect of steaming on (a) NO conversion to N_2 and (b) CH_4 conversion to CO_2 during SCR of NO by CH_4 over Ce(24)–Ag(77)-ZSM-5. The sample was steamed with 14.1% H_2O in He at 50 ml/min for 24 h prior to the SCR run. Feed gas: 0.5% NO–0.5% CH_4–2.5% O_2–He, S.V. = 7500 1/h. Symbol: ■: fresh, ●: 400°C-steamed, ▲: 500°C-steamed, ◆: 600°C-steamed.

3.1.2. Isothermal dry-wet cyclic tests

The performance of Ce–Ag-ZSM-5 in the presence and absence of water was also studied in an isothermal dry–wet cyclic mode at different temperatures and with different water contents over samples of various Ce and Ag loadings. Fig. 2 shows a run with the Ce(24)–Ag(78)-ZSM-5 sample at 500°C in a gas mixture of 0.5% NO, 0.5% CH_4, 0 or 4.1% H_2O, 2.5% O_2, bal. He at the space velocity of 7500 h^{-1}.

Upon addition of water into the feed gas stream, an immediate drop of both the NO conversion to N_2 and CH_4 conversion to CO_2 was observed. This initial fast drop was followed by a much slower, but continuous drop of the NO and CH_4 conversions until water was removed from the feed gas stream. After water was

Table 3
Catalyst performance in isothermal dry–wet cyclic tests[a]

	Catalyst	Temperature (°C)	H_2O (mol %)	Cycle-1 dry			Cycle-4 dry			Cycle-4 wet		
				NO to N_2 (%)	CH_4 to CO_2 (%)	Selectivity	NO to N_2 (%)	CH_4 to CO_2 (%)	Selectivity	NO to N_2 (%)	CH_4 to CO_2 (%)	Selectivity
1	Ce(24)–Ag(78)-Z	500	4.1	75	74	51	58	52	56	48	38	63
2	Ce(24)–Ag(78)-Z	500	8.3	74	72	51	38	45	42	30	20	75
3	Ce(24)–Ag(78)-Z	600	8.3	68	100	34	31	60	26	26	42	31
4	Ce(49)–Ag(79)-Z	500	8.3	82	75	55	40	40	50	32	25	65
5	Ce(21)–Ag(42)-Z	500	8.3	55	46	60	27	15	90	22	15	73

[a] (1) The feed gas mixture was 0.5% NO–0.5% CH_4–2.5% O_2–x% H_2O–He; S.V. = 7500 h^{-1}. (2) The selectivity was calculated on the basis of the stoichiometry: $2NO + CH_4 + 2O_2 = N_2 + CO_2 + 2H_2O$ for the SCR reaction.

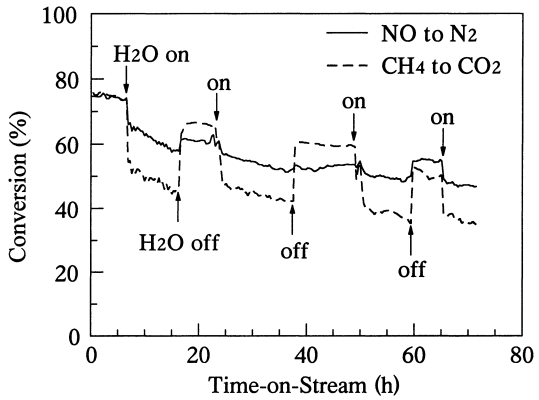

Fig. 2. Dry–wet cyclic test over Ce(24)–Ag(78)-ZSM-5 at 500°C. Feed gas: 0.5% NO–0.5% CH_4–2.5% O_2–0/4.1% H_2O–He, S.V. = 7500 h^{-1}.

removed, conversions were restored only partially, indicating some irreversible loss of catalyst activity. The same behavior was also observed in the second, third and fourth cycles, but with much smaller fluctuations, especially for the NO conversion which was stabilized at about 50% in the fourth cycle. Thus, the effect of water addition on the NO conversion to N_2 over the Ce–Ag-ZSM-5 catalyst consists of two segments: a rapid decrease followed by a much slower decline. The very different rates of these two types of deactivation imply that they might be controlled by different mechanisms. From Fig. 2, it can also be seen that the largest decrease in NO conversion (from 75% to 60%) occurred in the first cycle. This is true for other samples and at other conditions as will be shown later. The decrease of CH_4 conversion exceeds that of NO conversion in the presence of water vapor, as shown in Fig .2. Thus, in the presence of water, the selectivity of the catalyst was increased, e.g. more CH_4 was consumed by the SCR reaction. The catalyst selectivity in the first and fourth cycles is summarized in Table 3 for this and other runs. The improved catalyst selectivity at wet conditions may be caused by stronger adsorption of water on sites active for methane combustion. As reported before [16–19] and will be shown below, at least two states of silver, isolated Ag^+ ions and metallic Ag nanoparticles, exist in high Ag-loaded samples, such as Ce(24)–Ag(78)-ZSM-5. Ag^+ ions are more active for the SCR reaction while the (oxygen-covered) silver particles provide sites for methane combustion [17–19]. The data in Fig. 2 also show that CH_4 conversion recovers more than the NO conversion upon removal of water; we may attribute the reversible part of the profile to methane combustion recovery. As a result, the catalyst selectivity for the SCR reaction drops in the dry part of each cycle.

Fig. 3 shows the NO and CH_4 conversions in dry–wet cycles of CH_4-SCR over Ce(24)–Ag(78)-ZSM-5 at 500°C with 8.3% H_2O. The similarities to Fig. 2 are obvious. A larger drop in conversion of both NO to N_2 and CH_4 to CO_2 is caused by the higher content of water in Fig. 3. The very fast initial drop of conversion upon introduction of water, seen in both Figs. 2 and 3, is attributed to equilibrium adsorption of water. This increases with the water content. Similar effects have been reported for the Ce–Cu-ZSM-5 catalyst for the direct NO decomposition [12,13]. The slowly decreasing segment of the conversion profiles in Figs. 2 and 3 is attributed to gradual loss of sites due to structural changes. As will be discussed below, growth of silver particles is observed after wet gas-aging.

The same catalyst was examined under more severe operation conditions, i.e., at 600°C with 8.3% H_2O

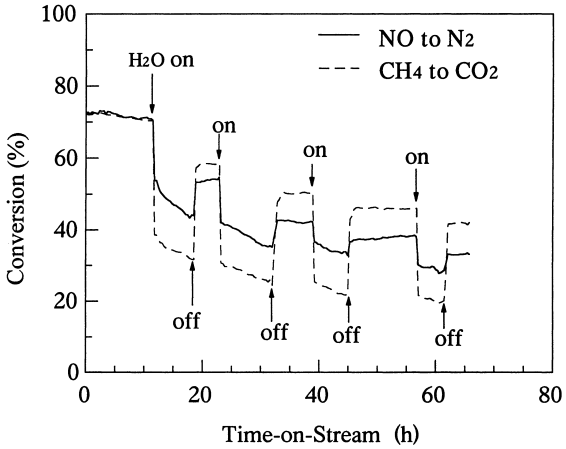

Fig. 3. Dry–wet cyclic test over Ce(24)–Ag(78)-ZSM-5 at 500°C. Feed gas: 0.5% NO–0.5% CH_4–2.5% O_2–0/8.3% H_2O–He, S.V. = 7500 h^{-1}.

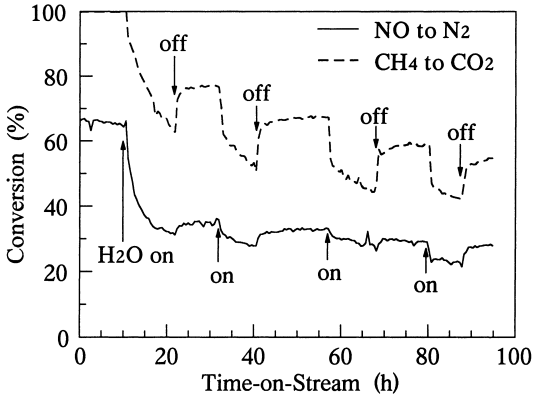

Fig. 4. Dry–wet cyclic test over Ce(24)–Ag(78)-ZSM-5 at 600°C. Feed gas: 0.5% NO–0.5% CH_4–2.5% O_2–0/8.3% H_2O–He, S.V. = 7500 h^{-1}.

content (Fig. 4 or Row 3 in Table 3), The initial fast drop of conversion increased under these conditions and the irreversible loss of catalyst activity dominated. In the first cycle, upon exposure of the catalyst to the wet gas mixture, the NO conversion to N_2 decreased rapidly from 68% to 55% and then slowly to about half of its initial dry-gas value. The overall decline over the first 10 h was much higher than that at 500°C and with 4.1% H_2O (Fig. 2). Subsequent removal or addition of water in the following cycles had little effect on the catalyst activity for the SCR reaction. However, the catalyst still retained a stable activity as shown by the 30–35% conversion of NO to N_2 after about 100 h on-stream at 600°C. The water-resistance

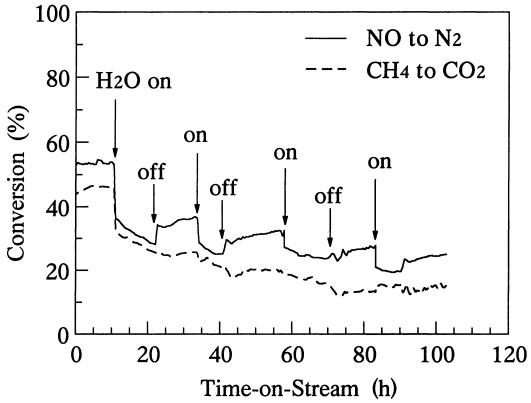

Fig. 5. Dry–wet cyclic test over Ce(21)–Ag(42)-ZSM-5 at 500°C. Feed gas: 0.5% NO–0.5% CH_4–2.5% O_2–0/8.3% H_2O–He, S.V. = 7500 h^{-1}.

of Ce–Ag-ZSM-5 is, comparable to that of Co-ZSM-5 [10,11].

The effect of cerium and silver loading on the dry–wet performance of Ce–Ag-ZSM-5 was also examined. As shown in Table 3, increasing the nominal cerium exchange level from 24% to 49% (1.05–2.1 wt.%, Table 3, rows 2 and 4, respectively), had little effect on the catalyst performance. However, lowering the silver exchange level alters the CH_4 conversion profile, while it leaves unaffected the NO conversion profile. As shown in Table 3 (rows 2 and 5), the percent drop in NO conversion to N_2 from first to fourth cycle is about the same. We have reported before that the absolute values of NO conversion are lower for samples with lower silver loading at all conditions, because the SCR rate increases with silver loading [16]. Comparing Figs. 3 and 5, we see that the CH_4 conversion profile over the low silver-content sample Ce(21)–Ag(42)-ZSM-5 is different from that over Ce(24)–Ag(78)-ZSM-5, showing no recovery upon removal of water. Structural differences between the two catalysts may explain the different CH_4 conversion profiles shown in Figs. 3 and 5. As shown below, the predominant state of silver in Ce(21)–Ag(42)-ZSM-5 is Ag^+ ions, while Ag^+ and metallic silver nanoparticles coexist in Ce(24)–Ag(78)-ZSM-5. Since silver particles provide sites for methane combustion, the absence of silver particles in Ce(21)–Ag(42)-ZSM-5 can explain the disappearance of the fluctuation of CH_4 conversion observed over the high Ag-loaded sample (Fig. 3).

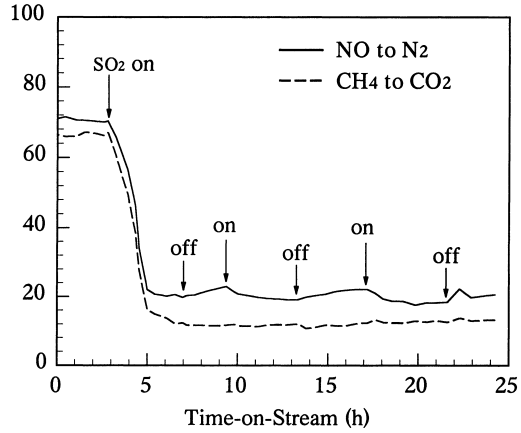

Fig. 6. SCR of NO by CH_4 over Ce(24)–Ag(78)-ZSM-5 at 500°C in the presence of SO_2. Feed gas: 0.5% NO–0.5% CH_4–2.5% O_2–(75 ppm SO_2)–bal. He, S.V. = 7500 h^{-1}.

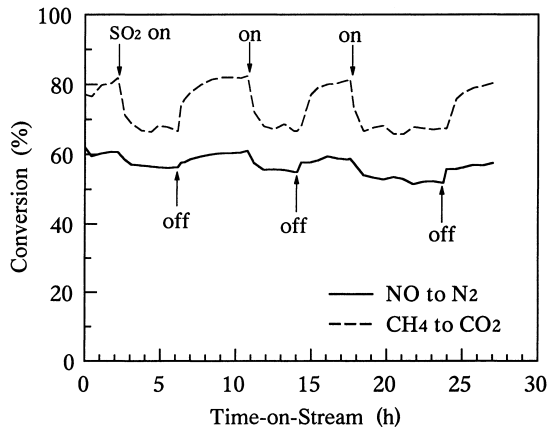

Fig. 7. SCR of NO by CH_4 over Ce(24)–Ag(78)-ZSM-5 at 600°C in the presence of SO_2. Feed gas: 0.5% NO–0.5% CH_4–2.5% O_2–(75 ppm SO_2)–bal. He, S.V. = 7500 h^{-1}.

3.2. Effect of SO_2 on the performance of Ce–Ag-ZSM-5

The conversions of NO and CH_4 over Ce(24)–Ag(78)-ZSM-5 in the presence of SO_2 are shown in Figs. 6 and 7 at 500°C and 600°C, respectively. At 500°C, addition of 75 ppm SO_2 into the dry gas mixture decreased the catalyst activity significantly. The conversions of NO and CH_4 dropped from an initial 65–70% to about 20% and 10%, respectively, 2 h after SO_2 was switched into the reactor in the first cycle. The presence of SO_2 had little effect on the selectivity, as indicated by the same reduction rate of the NO and CH_4 conversions. Addition or removal of the SO_2 in subsequent cycles did not change the conversions as shown in Fig. 6. However, at 600°C (Fig. 7), the presence of SO_2 had no appreciable effect on the NO conversion to N_2, while it decreased the CH_4 conversion by 15–20%. The latter effect was fully reversible, as shown in Fig. 7.

In a separate experiment, we further observed that the low NO and CH_4 conversions at 500°C in the presence of SO_2 could be restored to about 50% of the SO_2-free value as temperature was increased to 550°C. Complete recovery was again obtained at 600°C. Thus, SO_2 is merely an inhibitor of both the SCR and CH_4 oxidation sites of Ce–Ag-ZSM-5, but it does not cause permanent poisoning. Otherwise, permanent activity loss would have been seen. Similar behavior has been reported for Co-ZSM-5 [11], Co-FER [11] and Ag supported on alumina [24] catalysts. These findings can be contrasted to the effect of water vapor which causes permanent loss of catalyst activity at high temperatures.

SO_2 has been reported as a mild inhibitor of the SCR activity of Ag/Al_2O_3 and Ag/TiO_2–ZrO_2 catalysts with non-methane hydrocarbons or oxygenates used as reductants of NO [21,24,25]. No significant effect was measured above 400–450°C. However, in the present Ag-based catalyst the inhibition persists to higher temperatures, 550–600°C. We postulate that this is due to the presence of cerium in Ce–Ag-ZSM-5. Indeed, the nanoparticles of cerium oxide at the zeolite surface (see below) can be readily sulfated, even in the absence of oxygen, forming thermally stable cerous sulfate [27,28].

The performance of Ce(24)–Ag(78)-ZSM-5 in the presence of both H_2O and SO_2 was studied at the higher space velocity of 30 000 h^{-1} with a gas mixture of 0.1% NO, 0.2% CH_4, 2.5% O_2, 5% H_2O, 50 ppm SO_2, bal. He. The results are shown in Fig. 8 along with the data obtained at dry and SO_2-free conditions after 5 h at each temperature. At 500°C in the presence of both H_2O and SO_2, the conversion of NO is very low, around 10%, which is slightly less than the value of ∼15% reported for Co-ZSM-5 under similar conditions [11]. However, at 550°C the conversion of NO over Ce(24)–Ag(78)-ZSM-5 increased to 30% and 50% in the presence and absence of ($H_2O + SO_2$), respectively. These values are higher than the corresponding values obtained over Co-ZSM-5 under sim-

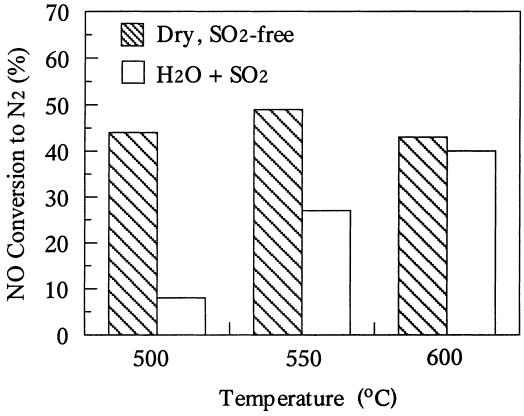

Fig. 8. SCR of NO by CH_4 over Ce(24)–Ag(78)-ZSM-5 in the presence of both H_2O and SO_2. Feed gas:1000 ppm NO–2000 ppm CH_4–2.5% O_2–(5% H_2O–50 ppm SO_2), S.V. = 30 000 h^{-1}.

ilar conditions (18% and 28%, respectively [11]). The difference between the NO conversion in the absence and presence of $H_2O + SO_2$ is smaller at 550°C than that at 500°C (see Fig. 8). This difference disappears at 600°C where the presence of $H_2O + SO_2$ has no effect on the conversion of NO to N_2 (Fig. 8). It is not clear why the presence of SO_2 moderates the water vapor effect on the catalyst. Competitive chemisorption of the two gases is a possible explanation. The higher CH_4/NO ratio (2 : 1) used for the tests shown in Fig. 8 may also have played a role.

3.3. Catalyst characterization

3.3.1. NO uptake over steamed and sulfated Ce–Ag-ZSM-5 catalysts

The effect of water vapor and SO_2 on the adsorption of NO was examined by measuring the NO uptake capacity of fresh, steamed and sulfated Ce(24)–Ag(78)-ZSM-5 at 300°C. Steaming or sulfation was performed at 400°C, 500°C or 600°C, followed by NO uptake at the lower temperature of 300°C in a cyclic adsorption–desorption mode to measure reversibly and irreversibly adsorbed NO. This is illustrated in Fig. 9 by the profiles of NO uptake versus time on the fresh Ce(24)–Ag(78)-ZSM-5 sample. The amounts of total, reversible and irreversible NO adsorption at various conditions are listed in Table 4. To better evaluate the effect of the pre-treatment, the percentage decrease of NO adsorption was calculated based on NO adsorption on the fresh sample. These values are also listed in Table 4.

Pre-treatment of the catalyst by steaming or sulfation decreases the amount of NO adsorption significantly, as shown in Table 4. However, the change of adsorption with pre-treatment temperature is totally different for the steamed and sulfated samples. As can be seen from Table 4, steaming of the catalyst at 400°C, 500°C and 600°C decreased the total amount of NO adsorbed by 20%, 48% and 89%, respectively, compared to the NO adsorption on the fresh sample. Thus, the higher the steaming temperature, the lower the total amount of NO adsorbed at 300°C. Furthermore, the percentage drop for the reversible and irreversible NO adsorption is approximately the same as that for the total adsorption, i.e. 19% and 22% versus 20% for the 400°C-steamed sample, 56% and 45% versus 48% for the 500°C-steamed sample and 90% and 89% versus 89% for the 600°C-steamed sample. Therefore, steaming was equally detrimental to all NO adsorption sites in the catalyst.

On the other hand, for the pre-sulfated samples, the total amount of NO adsorbed at 300°C increased with pre-treatment temperature. As measured in the TGA, this was accompanied by a lower amount of SO_2 remaining in the sample at the start of the NO adsorption step (after the 300°C-He purge). Thus, strong adsorption of SO_2 on the active sites is the major cause for the drop of NO uptake capacity of the catalyst. Over the 600°C-sulfated sample, the total NO adsorbed reached ~80% of the amount adsorbed on the fresh sample.

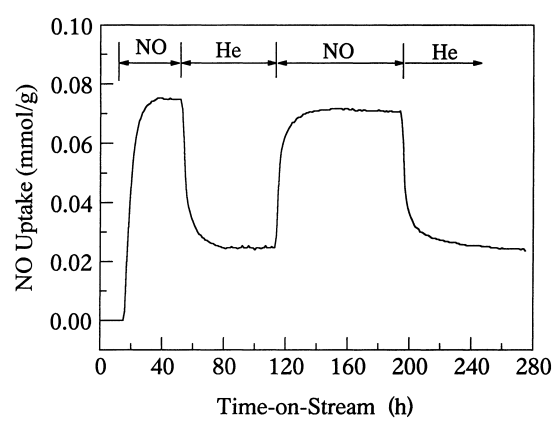

Fig. 9. NO uptake at 300°C by fresh Ce(24)–Ag(78)-ZSM-5. Adsorption gas: 0.2% NO in He, desorption gas: pure He, both at a flow rate of 100 cc min^{-1} (STP). Sample weight: ~10 mg.

Table 4
NO uptake at 300°C on fresh, steamed and sulfated Ce(24)–Ag(78)-ZSM-5[a]

Pre-treatment	Total		Irreversible		Reversible	
	mmol g^{-1}	% decrease	mmol g^{-1}	% decrease	mmol g^{-1}	% decrease
Fresh	0.0752	–	0.0247	–	0.0505	–
Steamed at 400°C	0.0596	20	0.0201	19	0.0395	22
Steamed at 500°C	0.0390	48	0.0110	56	0.0280	45
Steamed at 600°C	0.0081	89	0.0024	90	0.0057	89
Sulfated at 400°C	0.0259	66	0.0155	37	0.0104	79
Sulfated at 500°C	0.0407	46	0.0290	−17	0.0117	76
Sulfated at 600°C	0.0559	26	0.0287	−16	0.0272	46

[a] (1) Steaming was performed with 14.1% H_2O in He for 24 h. (2) Sulfation was performed with 500 ppm SO_2 in He for 1 h. (3) NO uptake was performed at 300°C with 4760 ppm NO in He at a flow rate of 100 cc min^{-1} (STP) after sample weight was stabilized in He purge at 300°C.

Also, as shown in Fig. 7, at this temperature there was no effect of SO_2 on the SCR activity. It has been reported that SO_2 can react with O_2 forming surface sulfate on Ag at temperatures above 200–300°C; decomposition of sulfate occurs at temperatures higher than 500°C over silver supported on alumina [24,29]. In the present catalyst, the cerium oxide component is also sulfated [27,28]. Due to its high thermal stability, cerous sulfate can explain the residual SO_2 even after the 600°C-treatment of the catalyst and the ensuing lower NO adsorption capacity (20% lower than that of the fresh catalyst, Table 4). This, however, does not impact the SCR activity of the catalyst at 600°C, Fig. 7.

3.3.2. XRD

X-ray diffraction patterns of the fresh, dry gas-aged and wet gas-aged Ce(24)–Ag(78)-ZSM-5 samples are shown in Fig. 10 along with a diffractogram for the wet gas-aged Ag(77)-ZSM-5. No metallic silver was detected when cerium was present in the samples. However, in the wet gas-aged, non-promoted Ag(77)-ZSM-5, metallic silver was found. It should be pointed out that metallic silver had not been detected by XRD in either the fresh or dry gas-aged Ag-ZSM-5 samples. Therefore, these results show that the presence of water vapor in the feed gas stream facilitated the formation of metallic silver in the non-promoted Ag-ZSM-5 catalyst, while cerium in the promoted catalyst prevents the formation of large particles of silver. Bulk silver oxides, Ag_2O and AgO, were not detected in either the Ce–Ag-ZSM-5 or Ag-ZSM-5 samples. Furthermore, cerium oxide species were not detected by XRD.

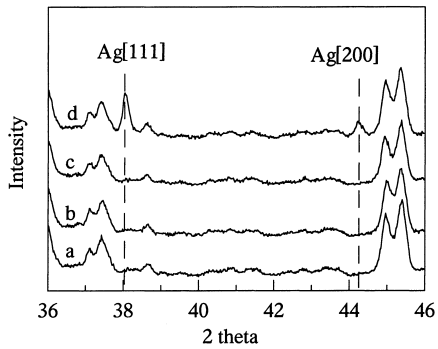

Fig. 10. XRD patterns of (a) fresh, (b) dry gas-aged, (c) wet gas-aged Ce(24)–Ag(78)-ZSM-5 and (d) wet gas-aged Ag(77)-ZSM-5. Fresh sample was air-calcined at 500°C for 2 h; dry gas-aged sample was exposed to 0.5% NO–0.5% CH_4–2.5% O_2–He at 500°C for 24 h; wet gas-aged sample was exposed to 0.5% NO–0.5% CH_4–2.5% O_2–14.1% H_2O–He at 500°C for 24 h.

3.3.3. HRTEM and STEM/EDX

HRTEM micrographs of fresh, dry gas-aged and wet gas-aged Ce(24)–Ag(78)-ZSM-5 are shown in Fig. 11(a)–(c), respectively. In the fresh sample (Fig. 11(a)), nanoparticles of 8–12 nm size as well as clusters of 1–3 nm are observed. EDS analysis of the 8–12 nm particles identified them as silver. Strong X-ray bands corresponding to silver and cerium were obtained in the areas where large silver particles are absent. In this case, the silver band may be due to X-ray emission from Ag^+ ions or clusters dispersed in the bulk of the zeolite particle. The 1–3 nm clusters located on the surface of the zeolite are probably Ce species, most likely in the form of oxidized CeO_x. Although CeO_2 was not identified by XRD, the presence of cerium species is supported by UV–Vis dif-

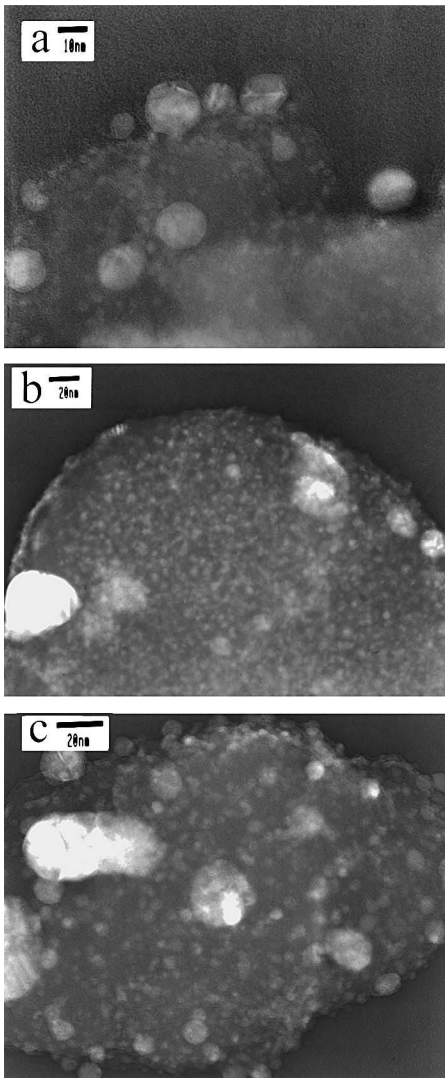

Fig. 11. HRTEM images of (a) fresh, (b)dry gas-aged and (c) wet gas-aged Ce(24)–Ag(78)-ZSM-5. Pre-treatment of the samples was the same as in Fig. 10.

fuse reflectance spectroscopy [16] and XPS analysis (see below). UV–Vis bands at 300, 196 and 210 nm corresponding, respectively, to cerium oxide and to dispersed Ce^{3+} species were obtained. Absorption at 300 nm has been assigned to charge transfer of cerium oxide clusters in the range of several nanometers (2–5 nm) in size by Rakai et al. [30] and Bensalem et al. [31].UV–Vis was also used to identify Ag^{+} ions in the zeolite [16]. Therefore, in the high Ag-loaded Ce(24)–Ag(78)-ZSM-5, silver exists both as isolated Ag^{+} ions and metallic nanoparticles. However, the same analytical techniques failed to identify metallic silver in the low Ag-loaded sample Ce(21)–Ag(42)-ZSM-5.

After dry gas-aging for 24 h (Fig. 11(b)), larger silver particles (20–40 nm) are observed on the catalyst surface, but the number density of these large particles is low, implying that the major portion of silver is still well dispersed. However, after wet gas-aging (Fig. 11(c)), the number of large particles (>10 nm) increased. In addition, many smaller silver particles in the size range of 5–10 nm are also clearly seen on the catalyst surface. Migration and sintering of silver on the catalyst surface during exposure of the sample to the wet gas can explain the gradual formation of different sized silver particles. It is known that silver is highly mobile in zeolites [32–34]. Of course, at 500°C in the presence of water, zeolite dealumination may also occur [12–16], which in turn can enhance silver migration/sintering. On the other hand, the cerium phase remains finely dispersed (1–3 nm clusters) even after wet gas-aging of the catalyst at 500°C for 24 h.

Elemental distributions of Si, Al, Ag and Ce in the wet gas-aged Ce(21)–Ag(42)-ZSM-5 and Ce(24)–Ag(78)-ZSM-5 are shown in the STEM/EDS micrographs of Fig. 12(a) and (b), respectively. The annular dark format (ADF) images in the figure show the areas where the elemental mappings were taken. In the low Ag-content sample Ce(21)–Ag(42)-ZSM-5 (Fig. 12(a)), the ADF image shows that silver particles (black spots) were formed after aging in the wet gas mixture at 500°C for 24 h. However, the Ag mapping in Fig. 12(a) shows that part of silver is still well dispersed. On the high silver-content sample, Ce(24)–Ag(78)-ZSM-5, formation of silver particles and enrichment of silver on the zeolite surface after wet gas-aging are evidenced by the big black spots in the ADF image and agglomerated Ag in the elemental mapping of Fig. 12(b). These results are consistent with the HRTEM results (Fig. 11(c)), i.e., water decreases the dispersion of silver in the Ce–Ag-ZSM-5 catalyst, especially in the high Ag-loaded sample.

Dispersed cerium as well as cerium oxide clusters are observed in both catalysts shown in Fig. 12(a) and (b). Compared to the previously reported structure of fresh and dry gas-aged samples [16], the distribution of cerium in wet gas-aged Ce–Ag-ZSM-5 samples remains the same, indicating that exposure to water va-

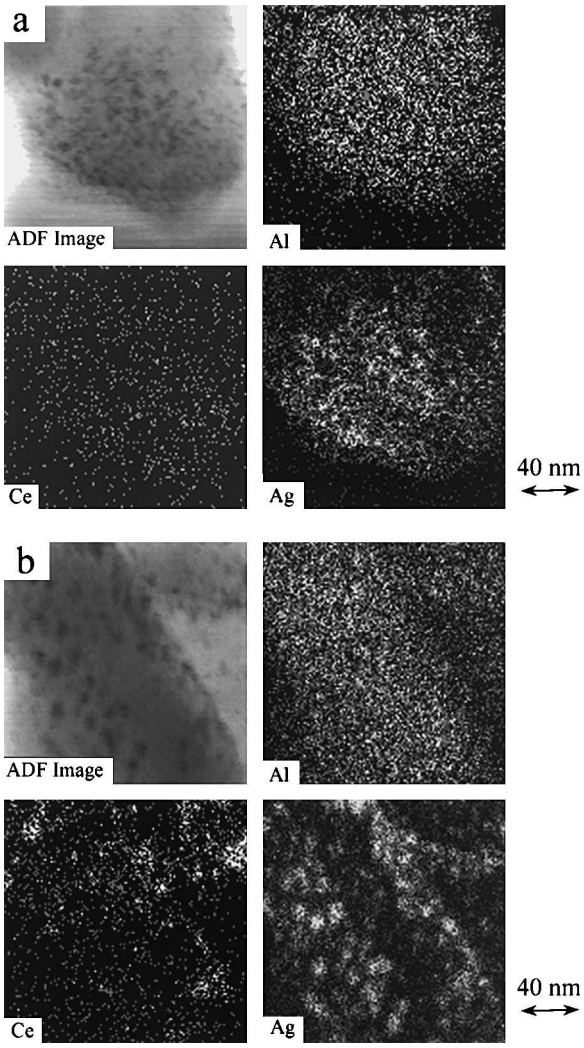

Fig. 12. STEM/EDS elemental mappings of wet gas-aged (a) Ce(21)–Ag(42)-ZSM-5 and (b) Ce(24)–Ag(78)-ZSM-5 samples. The samples were exposed to 0.5% NO–0.5% CH_4–2.5% O_2–14.1% H_2O–He at 500°C for 24 h.

por does not produce structural changes on the cerium component of the catalyst under the conditions examined here.

3.3.4. XPS

The atomic ratios of Ag/Si and Ce/Si in the surface region of the fresh, dry gas-aged and wet gas-aged Ce(24)–Ag(78)-ZSM-5 samples were measured by XPS. Data are shown in Fig. 13. Clearly, the surface Ag/Si ratio in the dry gas-aged sample does not

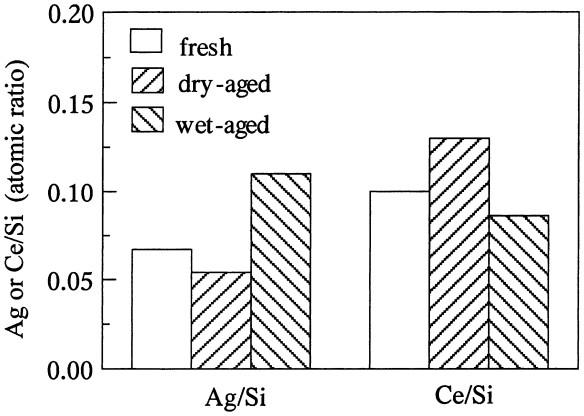

Fig. 13. XPS-measured atomic surface ratios of Ag/Si and Ce/Si in fresh, dry gas-aged and wet gas-aged Ce(24)–Ag(78)-ZSM-5. Pre-treatment of the samples was the same as in Fig. 10.

change very much compared to that in the fresh sample, but the Ag/Si ratio in the wet-aged sample is about twice that in either the fresh or dry gas-aged sample, i.e., 0.12 versus 0.06 or 0.05, showing surface enrichment of silver after the wet gas treatment. This is in agreement with the HRTEM and STEM/EDS analyses in Figs. 11 and 12.

The surface Ce/Si ratio in dry gas-aged Ce(24)–Ag (78)-ZSM-5 (0.13) is similar to that of the fresh (0.1) and wet gas-aged (0.08) samples. These values are much higher than the bulk Ce/Si ratio (0.005, based on ICP analysis), indicating the strong surface enrichment of cerium. Again, the XPS data are in agreement with the HRTEM and STEM/EDS analyses.

4. Summary

The activity and stability of Ce–Ag-ZSM-5 catalysts for CH_4-SCR of NO in the presence of water vapor and SO_2 were studied in this work. Steaming of the catalysts or addition of water vapor in the feed gas mixture decreased the catalyst activity. The loss of the catalytic activity was partially irreversible, and with an increase of water content and/or temperature, the irreversible loss became predominant. However, at all tested conditions, including at 600°C and with 8% water, the catalyst was capable of retaining a stable activity in 100 h-long testing.

Isolated Ag^+ ions and metallic silver nanoparticles coexist in the as prepared Ce–Ag-ZSM-5 catalysts, the

latter only at high silver loadings. The dispersed Ag^+ state is more active for the SCR reaction, while silver particles (5–12 nm, [17–19]) catalyze CH_4 combustion. Water induces migration and sintering of silver forming a wide range of particles (5–40 nm) on the zeolite surface causing the irreversible loss of catalyst activity for the SCR reaction. However, the presence of water had little effect on the structure of cerium, which exists in Ce–Ag-ZSM-5 mainly as dispersed cerium oxide clusters of 1–3 nm size.

In the presence of SO_2, the activity of Ce–Ag-ZSM-5 decreased significantly at 500°C. However, by raising the temperature to 600°C, the catalyst activity was fully restored. The inhibition by SO_2 at temperatures lower than 500°C is explained in terms of strong chemisorption and sulfate stability. No structural modifications due to SO_2were identified on the catalysts. In reaction tests at 550°C and 600°C with both SO_2 and H_2O present in the gas, the drop of SCR activity was not as large as in H_2O-only tests. The reasons for this are being explored in work currently underway.

Acknowledgements

We gratefully acknowledge the financial support of this work by US EPA under Grant No. R825430-01-0. We also thank Dr. Anthony Garratt-Reed, Mr. Michael Frongillo and Ms. Elisabeth Shaw of the Center of Materials Science and Engineering at the Massachusetts Institute of Technology for their assistance with the STEM/EDS, HRTEM and XPS analyses. We also appreciate the comments of the reviewers of this paper.

References

[1] Y. Li, J.N. Armor, U.S. Patent 5,149,512, 1992.
[2] Y. Li, J.N. Armor, Appl. Catal. B: Environ. 1 (1992) L31.
[3] Y. Li, J.N. Armor, J. Catal. 145 (1994) 1.
[4] E. Kikuchi, M. Ogura, N. Aratani, Y. Sugiura, S. Hiromoto, K. Yogo, in: G. Centi, S Perathoner, C. Christani and P. Forzatti (Eds.), Environmental Catalysis, Rome, Italy, 1995, p. 29.
[5] K. Yogo, E. Kikuchi, Stud. Surf. Sci. Catal. 84 (1994) 1547.
[6] X. Zhou, T. Zhang, Z. Xu, L. Lin, Catal. Lett. 40 (1996) 35.
[7] C. Descorme, A. Fakche, E. Garbowski, M. Primet, Proc. 1995 Int. Gas Res. Conf., 1995, p. 505.
[8] C.J. Loughran, D.E. Resasco, Appl. Catal. B: Environ. 7 (1996) 127.
[9] Z. Li, M. Flytzani-Stephanopoulos, Appl. Catal. A: General 165 (1997) 15.
[10] Y. Li, P.J. Battavio, J.N. Armor, J. Catal. 142 (1993) 561.
[11] Y. Li, J.N. Armor, Appl. Catal. B: Environ. 5 (1995) L257.
[12] Y. Zhang, Sc.D. Thesis, MIT, Cambridge, MA, 1995
[13] Y. Zhang, M. Flytzani-Stephanopoulos, J. Catal. 164 (1996) 131.
[14] A. Kucherov, C.P. Hubbard, M. Shelef, J. Catal. 157 (1995) 603.
[15] R.A. Grinsted, H.W. Jen, C.N. Montreuil, M.J. Rokosz, M. Shelef, Zeolites 13 (1993) 602.
[16] Z. Li, M. Flytzani-Stephanopoulos, J. Catal. 182 (1999) 313.
[17] Lj. Kundakovic, Ph.D. dissertation, Tufts University, Medford, MA, 1998
[18] Lj. Kundakovic, M. Flytzani-Stephanopoulos, J. Catal. 179 (1998) 203.
[19] Lj. Kundakovic, M. Flytzani-Stephanopoulos, Appl. Catal. A: General, in press.
[20] T. Miyadera, Appl. Catal. B: Environ. 2 (1993) 199.
[21] Miyadera, T., Yoshida, K., Chem. Lett. (1993) 1483.
[22] K.A. Bethke, H.H. Kung, J. Catal. 172 (1997) 93.
[23] T.E. Hoost, R.J. Kudla, K.M. Collins, M.S. Chattha, Appl. Catal. B: Environ. 13 (1997) 59.
[24] A. Abe, N. Aoyama, S. Sumiya, N. Kakuta, K. Yoshida, Catal. Lett. 51 (1998) 5.
[25] M. Haneda, Y. Kintaichi, M. Inaba, H. Hamada, Bull. Chem. Soc. Jpn. 70 (1997) 499.
[26] K. Masuda, K. Shinoda, K. Tsujimura, Appl. Catal. B: Environ. 15 (1998) 29.
[27] T. Zhu, A. Dreher, M. Flytzani-Stephanopoulos, Appl. Catal. B: Environ., in press.
[28] M. Waqif, P. Bazin, O. Saur, J.C. Lavalley, G. Blanchard, O. Touret, Appl. Catal. B: Environ. 11 (1997) 193.
[29] D.A. Outka, R.J. Madix, Surf. Sci. 137 (1984) 242.
[30] R. Rakai, A. Bensalem, J.C. Muller, D. Tessier, F. Bozon-Verduraz, Proc. 10th Int. Congress on Catalysis, 19–24 July 1992, Budapest, Hungary, pp. 1875–1878.
[31] A. Bensalem, F. Bozon-Verduraz, M. Delamer, G. Bugli, Appl. Catal. A: General 121 (1995) 81.
[32] N.E. Bogdanchikova, M.N. Dulin, A.V. Toktarev, G.B. Shevnina, V.N. Kolomiichuk, V.I. Zaikovskii, V.P. Petranovskii, Stud. Surf. Sci. Catal. 84 (1994) 1067.
[33] N.E. Bogdanchikova, M.N. Dulin, A.V. Toktarev, G.B. Shevnina, V.N. Kolomiichuk, V.I. Zaikovskii, V.P. Petranovskii, React. Kinet. Catal. Lett. 49 (1993) 87.
[34] E. Gachard, J. Belloni, M.A. Subramanian, J. Mater. Chem. 6 (1996) 867.